

Local probing of the surface chemical bond using X-ray emission spectroscopy

A. Nilsson¹, N. Wassdahl¹, M. Weinelt¹, O. Karis¹, T. Wiell¹, P. Bennich¹, J. Hasselström¹, A. Föhlisch¹, J. Stöhr², M. Samant²

¹Department of Physics, Uppsala University, Box 530, S-751 21 Uppsala, Sweden

²IBM Research Division, Almaden Research Center, 650 Harry Road, San Jose, California 95120-6099, USA

Accepted: 6 March 1997

Abstract. X-ray emission spectroscopy applied to adsorbate systems is shown to reveal new details of the chemical bond formed at surfaces. An atom and symmetry projected view of the bonding orbitals is obtained. We will present recent studies of N₂ and CO on Ni(100), benzene on Ni(100) and Cu(110), and glycine adsorbed on Cu(110). New types of molecular states are observed which are directly related to the surface chemical bond. The long-accepted Blyholder model which is based on a frontier orbital concept cannot explain our results for N₂ and CO chemisorption. We find it necessary to offer a new picture where changes in the whole molecular orbital framework have to be considered. We show that both π and σ type interactions are important in describing the bonding in benzene to metal surfaces. The future prospect is illustrated by the adsorption of the simplest amino acid, glycine, on Cu(110). The adsorbate has four different atomic centers where X-ray emission spectra are obtained, providing a unique view of the local electronic structure.

PACS: 78.70.En; 73.20.Hb; 85.65.Pa

When a molecule is adsorbed on a metal surface by chemical bonding new electronic states are formed. The direct observation and identification of these states is still an experimental challenge. For noble and transition metal surfaces, the adsorption-induced states overlap with the metal d valence band. Their signature is therefore often obscured by bulk substrate states. This complication has made it difficult for techniques such as photoemission and inverse photoemission to provide reliable information on the energy of chemisorption induced states and has left questions unanswered regarding the validity of different theoretical models.

In the following contribution we will show how X-ray emission spectroscopy (XES), in spite of its inherent bulk sensitivity, can be used to investigate adsorbed molecules [1–5]. Due to the localization of the core-excited intermediate state, XE spectroscopy allows an atom-specific separation of

the valence electronic states. Thus the molecular contributions to the surface chemical bond can be separated from those of the substrate. Furthermore, angle-dependent measurements make it possible to determine the symmetry of the molecular states, i.e. the separation of π and σ type states [4]. In all we can obtain an atomic view of the electronic states involved in the formation of the chemical bond to the surface.

Photon-excited X-ray emission should in the general case be treated as a one-step process and this is conveniently done within a scattering framework (see, for example, contributions in these proceedings dealing with resonant inelastic X-ray scattering (RIXS)). In many cases, however, excitation and decay can be treated as separable events. A fully adequate description can thus be provided within the traditionally used two-step picture, where in the first step a core hole is created by an electron transition from a core level to either a bound empty valence level or to the ionization continuum, and in the second step, the core hole is filled by an electron from an occupied valence level under emission of X-rays. Both steps are normally described within the dipole approximation which implies that the filling of the 1s level in systems containing C, N, and O will give only 2p contributions to the XE spectra. Furthermore, since the 1s level is localized on one atomic site, the transition matrix element will be dominated by the 2p contribution on that particular atom.

In a one-electron picture the XE spectrum reflects the occupied valence electron states. However, it is important to consider the influence of the core holes involved in the process. This influence has been summarized in the so-called “initial and final state rules” for X-ray spectroscopies [6–9]. The final state rule states that the spectral features reflect the eigenstates of the final state Hamiltonian. In XES, the core hole is filled by a valence electron leading to a final state related to the ground state. The final state in XES contains the quasiparticle valence hole similar to the final state in valence band photoemission. The position of the Fermi level in the spectrum, to which the valence electron states are related, is provided by the core level photoemission binding energy [10]. The initial state rule states that the integrated intensity in the spectrum is determined by the initial state of the transition. In XES, it contains a core hole and the *inte-*

International Workshop “Resonant Inelastic Soft X-ray Scattering (RIXS)”, Walberberg, 5–7 September 1996

grated spectral intensity therefore reflects the total number of occupied states in the presence of the core hole. Since we are only interested in relative intensities between different spectral features within one spectrum and not the total intensity, the core hole effect vanishes within the description of these simple rules. However, there are corrections to the final state rule due to dynamical effects in the deexcitation process which could affect the relative intensities. Recent theoretical model calculations of the XE process in adsorbates give no significant modification of the interpretation using ground state frozen orbitals or a fully relaxed core hole state, respectively [11]. There are only minor changes of the relative intensities except for a model-induced strong state close to the Fermi level in the fully relaxed core hole state calculation.

If the photon energy in the first step is far above the excitation threshold there is a large probability of creating multi-electron excited states. These are normally seen as shake-up and shake-off satellites in core level photoemission spectra. The presence of additional initial states for the decay process gives rise to X-ray satellites and these can have a substantial overlap in energy with the diagram lines. This will in turn make the assignment of the “one-electron states” difficult. However, by using threshold excitation the multiply excited states can be suppressed and a clean initial state for the decay can be produced. This requires a tuneable synchrotron radiation source.

The presence of an extra electron above the Fermi level in a threshold-excited decay process could in principle modify the spectra. This is utilized in RIXS and has recently been addressed in a large number of studies of solids and free molecules (see other contributions in these proceedings). For these systems very large spectral changes can be seen with varying excitation energy. For chemisorbed systems, on the other hand, one can expect the effects to be much smaller since the excited electron can couple to the continuum of metal states and becomes delocalized. In fact, the spectral profiles obtained in resonant Auger measurements of chemisorbed systems are essentially independent of excitation energy [12, 13]. The excited state is regarded as locally identical to the metallic screened core level ionization state. We can therefore assume that the presence of the excited electron has a negligible influence on the X-ray emission process and the spectra can be interpreted in a two-step picture with a fully relaxed initial core hole state.

In free molecules with inversion symmetry there exists, as a consequence of the dipole approximation, a parity selection rule [14, 15]. The electronic states in such molecules have either *gerade* (g) or *ungerade* (u) symmetry with respect to the inversion center. When the core electron is excited to an empty state of a particular symmetry only valence hole states of the same symmetry are seen in the XE spectrum. If, upon chemisorption, the inversion symmetry is only weakly perturbed, the selection rule will still have some influence on the transition intensities and this can be used to assign the molecular symmetry of new electronic states created due to the molecule–surface interaction.

For oriented systems the symmetry of the states can be obtained from angle-dependent measurements [4]. As an illustration we consider CO, which adsorbs with the molecular axis perpendicular to the surface. In the X-ray absorption process the linearly polarized incident radiation leads to $1s\text{-}\sigma$ ($1s\text{-}\pi$) transitions if the E -vector is parallel (perpendicular)

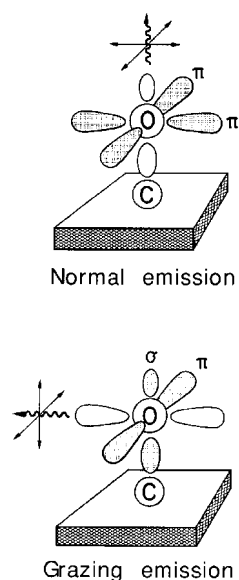


Fig. 1. The experimental geometries for adsorbed CO. For normal emission only π contributions are seen, while the grazing emission spectrum contains both σ and π contributions

to the molecular axis, respectively [4]. The same symmetry rules also hold for the emitted X-rays. However, since we do not analyze the polarization of the emitted X-rays, symmetry information only comes from the fact that the E -vector is always perpendicular to the direction of the emitted X-rays. In Fig. 1 we show the two different experimental geometries necessary for symmetry-selective detection of the emission from adsorbed CO (only emission from the oxygen atom is indicated in the figure). In the case of normal emission we probe transitions from the two degenerate π orbitals to the $1s$ core hole, whereas in grazing emission transitions from one of the π orbitals and the σ orbital are seen. This means that orbitals with pure π -symmetry are observed in normal emission and in grazing emission both π and σ orbitals are probed. The σ orbitals can then be obtained by a subtracting procedure where we assume equal contributions from both types of orbitals in the grazing emission spectrum.

1 Experimental considerations

XES applied to monolayers on surfaces is experimentally very demanding, and it is only recently that the field has begun to be exploited, mainly due to the appearance of third-generation synchrotron radiation sources. The main concern is the count rate and there are three effects acting together: (i) with only one sample layer the target density for the exciting beam is very low; (ii) most of the core holes that are created in the layer will decay by nonradiative processes (in the case of C, N, and O $1s$ hole states, only about 0.1% decay by X-ray emission); (iii) only a small fraction (about 10^{-8}) of the emitted photons are actually detected. This is mainly due to the inherently small acceptance angle of high-resolution grating instruments (in other respects the best ones for the purpose). With these effects taken together it is clear that experiments of this kind require a highly efficient excitation source. In principle, electron excitation could be used but in general the electron beam would be far too destructive for the sensitive molecular adsorbate systems. Furthermore, as discussed above, it is essential to use threshold excitation

in order to avoid satellites. Thus, monochromatic synchrotron radiation is the best choice. In order to have a reasonable count rate a photon flux of the order of 10^{13} to 10^{14} photons per second is required on the sample within a $100\ \mu\text{m}$ spot. The experiments in the present contribution have been carried out at the Advanced Light Source (ALS) using beamline 8.0 which is based on a undulator with 98 5-cm periods and a spherical grating monochromator.

The X-ray emission spectra were recorded using a multi-grating, grazing incidence spectrometer with a movable multichannel-plate-based detector, described in detail elsewhere [16]. To allow for angle-resolved measurements the spectrometer was rotatable around the axis of the incoming beam. The C K emission spectra were measured using a $400\ \text{lines}\ \text{mm}^{-1}$ grating and the N and O K emission spectra with a $1200\ \text{lines}\ \text{mm}^{-1}$ grating, both with a spherical radius of 5 m. The resolution was typically set to $0.5\text{--}0.6\ \text{eV}$. It is essential to have a reliable method for energy calibration. By setting the monochromator to different (well-defined) excitation energies and reflecting the beam into the spectrometer, a common energy scale for the monochromator and the spectrometer was established. With this procedure an accuracy of the order of $\pm 0.1\ \text{eV}$ was typically obtained.

The large penetration depth of the photons gives an inherently low surface sensitivity of the X-ray probe, as indicated above. The surface signal can, however, be substantially improved by operating with small angles ($3\text{--}5^\circ$) between the incident beam and the surface (there are no problems with separation from the bulk since the element under study in the adsorbate only exists on the surface) [1]. For many molecular adsorbates the high-intensity beam is very destructive. In these cases it is necessary to scan the sample in front of the spectrometer.

2 Applications to adsorbate systems

2.1 CO and N₂ adsorbed on Ni(100)

CO and N₂ adsorbed on the late transition metals have become prototype systems for the general understanding of molecular adsorption. It is in general assumed that the bonding of molecules to transition metals can be explained in terms of the interaction of the frontier molecular orbitals with the d orbitals. The frontier orbitals are the HOMO and LUMO molecular orbitals. In such a picture the other molecular orbitals should remain essentially the same as in the free molecule. For the adsorption of the isoelectronic molecules CO and N₂ this has led to the so-called Blyholder model, i.e. a synergetic σ (HOMO) donor and π (LUMO) backdonation bond [17]. Our recent results show that such a picture is oversimplified [5].

It is important not only to observe new electronic states related to the surface chemical bond but also to study changes in the contribution from different atoms to the molecular orbitals upon adsorption. The upright adsorption geometry of the N₂ molecule on Ni(100) in an on-top site leads to two chemically inequivalent N atoms. If a separation between the two atoms can be made it is an ideal opportunity for studying how the electronic states redistribute in a homonuclear molecule upon adsorption.

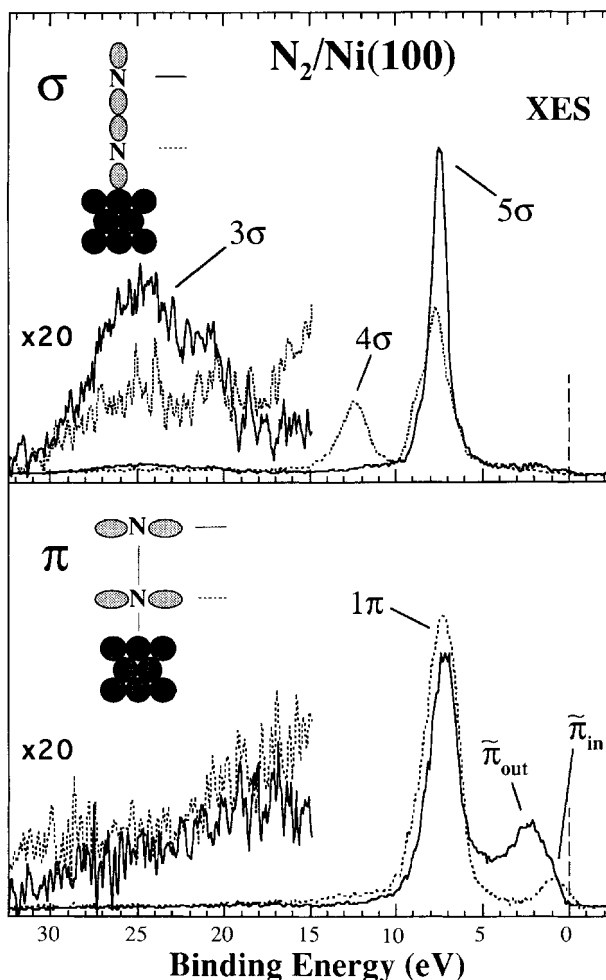
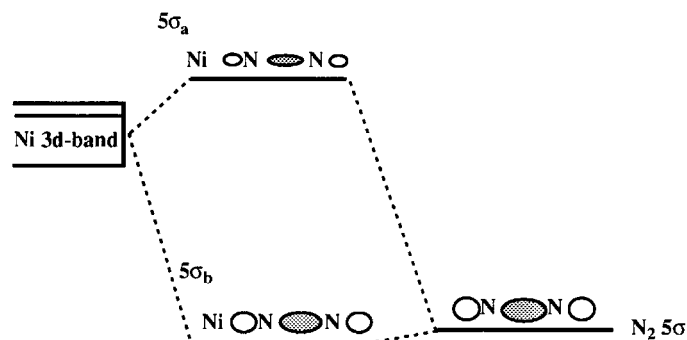
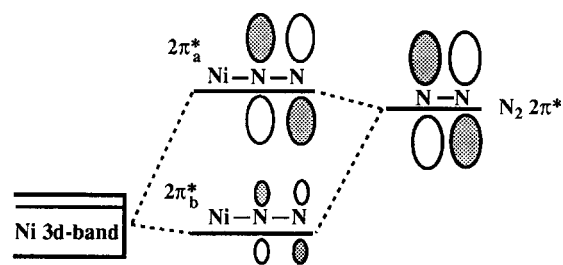


Fig. 2. Symmetry-resolved X-ray emission spectra for the inner and outer N atoms for N₂/Ni(100). The two N atoms were separated by selective X-ray excitation at 400.6 eV (outer atom) and 401.0 eV (inner atom). Peaks in the spectra are labeled by the corresponding molecular orbitals. New orbitals arising from the surface chemical bond are indicated by a tilde symbol

Previous work has shown that the X-ray absorption spectrum for N₂ on Ni(100) exhibits two $1s$ to $2\pi^*$ resonances at 400.6 and 401.0 eV [18], corresponding to the outer and inner N atoms, respectively. Hence, by using different excitation energies, site-specific XE spectra can be recorded. The resulting XE spectra for the outer and inner N atoms are shown in Fig. 2. The spectra are plotted on a common binding energy scale relative to the Fermi level, obtained by subtracting the N $1s$ core-level photoemission binding energies of the two atoms (outer atom: 399.4 eV; inner: 400.7 eV [19]) from the emission energies [10]. The figure is divided in an upper part, displaying states of σ symmetry (obtained by subtracting the grazing emission spectra from a normal emission spectrum scaled by 0.5) and a lower part, displaying states of π symmetry (the normal emission spectra). From the symmetry and binding energies of the spectral features, it is straightforward to assign all features above 5 eV binding energy by analogy with UPS measurements [20, 21]. In order to facilitate the comparison with the much-studied CO molecule we shall use the symmetry notation $C_{\infty v}$ for the molecular orbitals.

The novel information contained in Fig. 2 is the large difference in the states located on the inner and outer N atoms

Blyholder Model



New Model

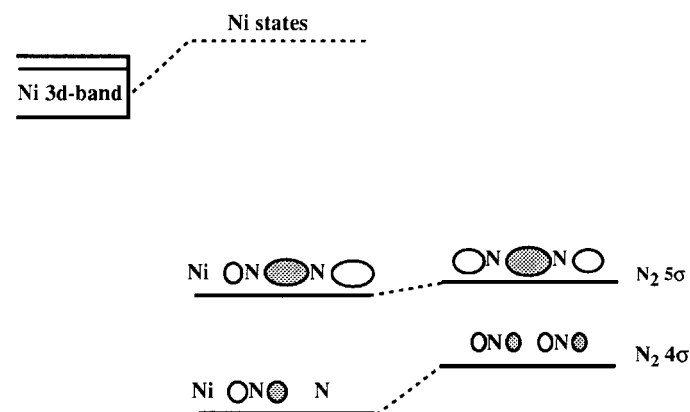
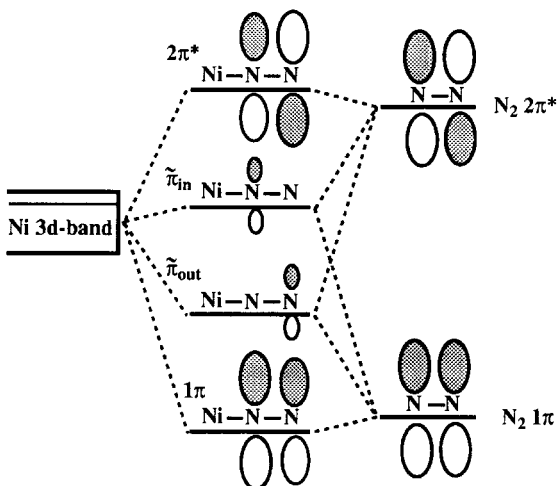


Fig. 3. Schematic illustration of the interactions of the π orbitals (left), and σ orbitals (right), with the Ni 3d band for the $N_2/Ni(100)$ system in the Blyholder model (upper pane) and based on our new results (lower pane)

and the clearly resolved structures within 5 eV binding energy, i.e. in the Ni d band region. All spectral peaks, representing the 2p atom-projected molecular orbitals, exhibit different intensities or shapes for the inner and outer N atoms. Even the 3σ , located about 25 eV below the Fermi level, shows an intensity difference for the two atoms, demonstrating that the chemisorption bond affects even the inner valence levels. Other interesting findings are the localization of the 4σ state to the inner N atom, with no visible spectral intensity from the outer N atom, and the larger 5σ localization to the outer N atom. Near the Fermi level we find the molecular states which are important for the surface chemical bond. These states arise from interaction of molecular π states, as discussed below, with the Ni d states. The state located on the outer N atom is centered at about 2.5 eV binding energy while the state located on the inner N atom is centered at about 1 eV.

In Fig. 3, we show in a schematic illustration how our new findings can be compared with the Blyholder model, where the surface chemical bond is described by 5σ donation into the substrate and a backdonation of d states into the empty molecular $2\pi^*$ orbital. In a molecular orbital picture the 5σ and $2\pi^*$ interactions would lead to a splitting into bonding and antibonding states as shown in Fig. 3. The molecular character is large for the occupied 5σ bonding states and small for the antibonding states. The reverse will hold for the

$2\pi^*$ -3d hybrid states, reflecting the difference in energy position of the 5σ orbital and $2\pi^*$ relative to the Ni 3d band. It is assumed that the atomic population on the two atoms in the new adsorbate states resembles those of the free molecule. This is not what we see in our spectra. Instead we observe the appearance of two new states, $\tilde{\pi}_{in}$ and $\tilde{\pi}_{out}$. These states are nonbonding with respect to the N-N bond and do not have much resemblance to the original orbitals of the free molecule. We can only generate these states through a linear combination of the original 1π and $2\pi^*$ orbitals. We picture the $\tilde{\pi}_{in}$ state to be strongly Ni-N bonding whereas the $\tilde{\pi}_{out}$ state is essentially a N 2p lone pair. It may contain some nonbonding Ni contribution [5].

In the spectra we do not see any new occupied states of 5σ symmetry and in previous XA spectra of adsorbed N_2 there are no indications of any new states above the Fermi level [22]. Thus we do not observe any bonding and antibonding states, indicating a significant 5σ contribution to the surface chemical bond. This supports the cluster calculations of Bagus and Pacchioni [23], which show the σ contribution to be mainly repulsive. Our spectra show the repulsion effects as a redistribution of the molecular σ system upon formation of the surface chemical bond. The 4σ state becomes polarized on the inner and the 3σ and 5σ states on the outer nitrogen atoms. Surprisingly, all valence states, down to the 3σ state

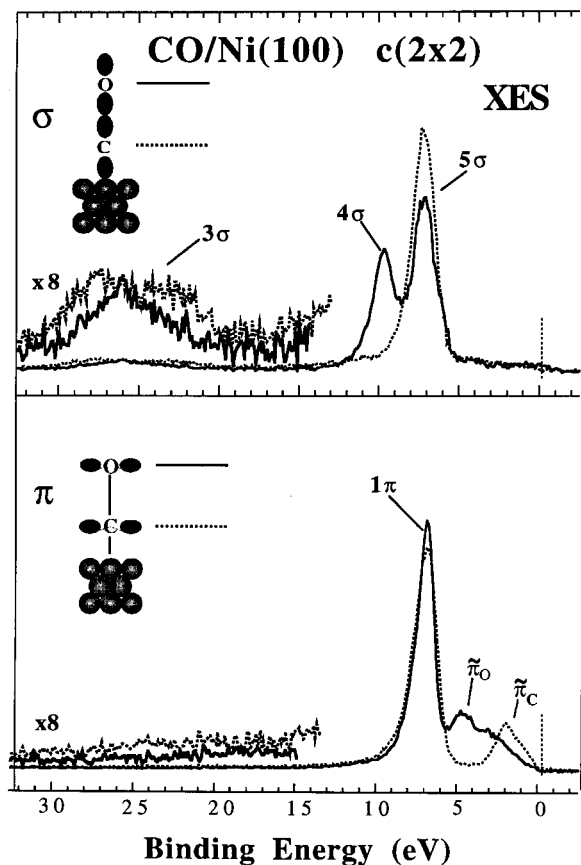


Fig. 4. Symmetry-resolved X-ray emission spectra for the C atom and O atom for CO/Ni(100). Peaks in the spectra are labelled by the corresponding molecular orbitals. New orbitals arising from the surface chemical bond are indicated by a tilde symbol

around 25 eV binding energy, are affected by the formation of the chemisorption bond. Despite the relative weakness of the chemisorption bond (≈ 0.4 eV) relative to the intramolecular bond (≈ 8 eV) the intramolecular bonding is completely changed upon chemisorption.

The isoelectronic CO molecule adsorbs in the same way as N_2 in an on-top site with the carbon end down. In this case the chemisorption bond is much stronger (≈ 1.5 eV). Figure 4 shows the XE spectra for the carbon and oxygen atoms on a common binding energy scale relative to the Fermi level (C 1s 285.9 eV and O 1s 532.2 eV [24]). The upper part shows states of σ symmetry while the lower part shows states of π symmetry. All spectral features with a binding energy above 5 eV has been observed previously with UPS [25]. We observe that the 5σ state is mainly located at the inner carbon atom and the 4σ on the outer oxygen atom. At first sight this appears to be the reverse situation compared with N_2 . However, the distribution of the molecular orbitals in the free molecule is very different. In the oxygen XE spectrum of free CO the intensity of the 4σ state is about five times larger than the 5σ [27]. From Fig. 4 we can observe that upon adsorption the intensity of the 5σ state becomes slightly larger than the 4σ . The 5σ slightly redistributes itself in the same manner as seen in adsorbed N_2 due to the repulsive interaction with the substrate. The 4σ state stays completely localized on the outer oxygen atom as in the free molecule. In the π system we

also observe two new states, $\tilde{\pi}_C$ (C–Ni bonding state) on the inner carbon atom and $\tilde{\pi}_O$ (O lone pair state) on the outer oxygen atom similar to N_2 . The energy splitting between the two states is larger in CO than in adsorbed N_2 : 3 eV and 1.5 eV, respectively. This can be attributed to the energy difference of the atomic 2p levels in carbon and oxygen. As can be seen in the oxygen XE spectrum, the $\tilde{\pi}_C$ state is not entirely localized on the carbon atom. The observed changes in the π system upon chemisorption resemble those between free CO and H_2CO . When two hydrogen atoms are added to CO to form H_2CO one of the π orbitals breaks up into a local C–H bonding orbital ($1b_1$) and an O 2p nonbonding lone pair orbital ($2b_1$), by analogy with the inner π and outer π states in both adsorbed CO and N_2 .

The two adsorption examples above nicely demonstrate how oversimplified a frontier orbital concept is for the description of surface chemical bonding. The bond is not only related to the appearance of new orbitals, it is also important to consider changes in the complete molecular orbital framework. The resulting electronic structure of the chemisorption complex is well described in an atom-based picture which X-ray emission spectroscopy (XES) provides.

2.2 Benzene adsorbed on Cu(110) and Ni(100)

We now move to adsorption of aromatic hydrocarbons. Benzene has for a long time served as a prototype adsorption system of large molecules. It adsorbs with the molecular plane parallel to the surface. The bonding of benzene to a transition metal is typically thought to involve the π system. The π –substrate interaction could be expected to be different compared with CO and N_2 since the π system is now parallel to the surface and we expect each carbon system to contribute equally to all states (unless there is strong variation in the substrate leading to different local carbon–substrate interactions). Benzene adsorbs weakly on Cu and strongly on Ni. It is interesting to study how the adsorption strength is reflected in the electronic structure of the adsorbate–substrate complex.

XE and XA spectra for benzene on Cu(110) and Ni(100) are shown in Figs. 5 and 6 [5, 28]. XE spectra were taken at an excitation energy corresponding to the C 1s to $\pi^*(e_{2u})$ transition. The spectra are plotted on a photon energy as well as valence hole binding energy scale (C 1s binding energies of 284.1 eV and 284.9 eV for benzene adsorbed on Ni and Cu, respectively). The assignment of the XE features with binding energies larger than 4 eV is known from the literature and it is given in the figures for the π system [14, 29]. The pronounced polarization dependence of the XA spectrum shows that benzene is adsorbed with the molecular plane parallel to the surface [30]. Based on this adsorption geometry, the XE spectra shown in Figs. 5 and 6 corresponding to pure σ and π symmetries were obtained in the same way as described earlier for CO and N_2 .

If we start with states of π symmetry (dashed lines) we find three distinct peaks. The $1a_{2u}$ and $1e_{1g}$ π -like orbitals are essentially intact from the gas phase, while the third state, labeled e_{2u} , is not seen for the free molecule. The inversion symmetry of the molecule seems to be partly conserved upon adsorption [28]. It was shown that peaks corresponding to *gerade* or *ungerade* symmetry states changed their relative intensity depending on the symmetry of the excited intermediate state. The spectra in Figs. 5 and 6 correspond to

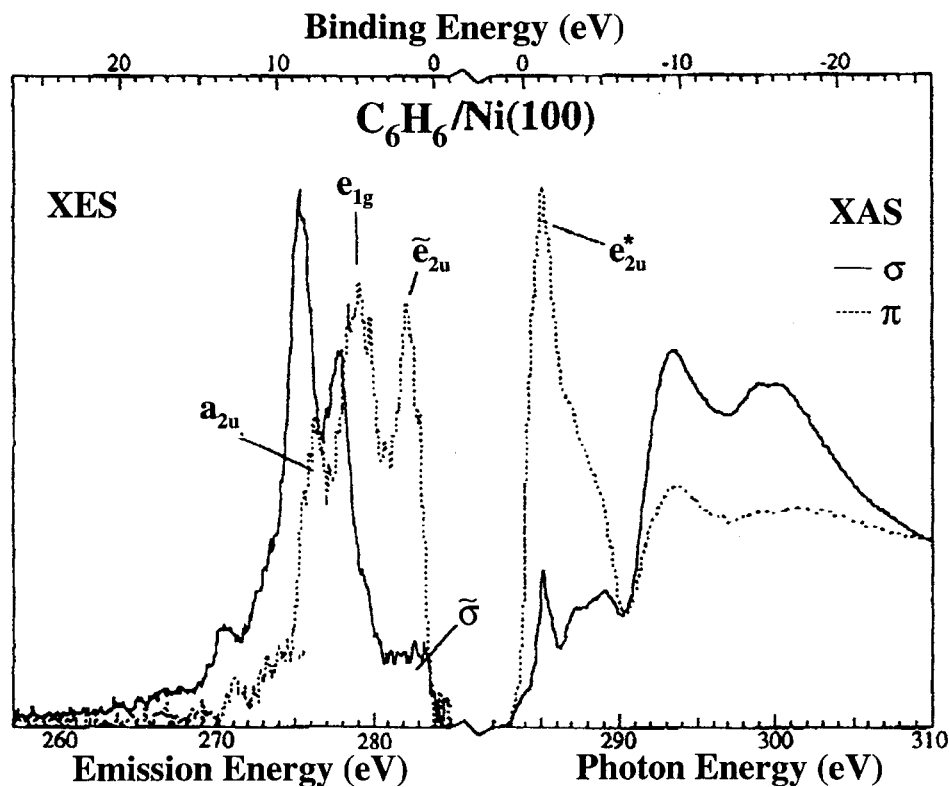


Fig. 5. Symmetry resolved X-ray emission and X-ray absorption spectra for benzene on Ni(100). The π symmetry peaks in the spectra are labeled by the corresponding molecular orbitals, empty states being designated by an asterisk. New orbitals arising from the surface chemical bond are indicated by a tilde symbol

a (u) excited state and therefore peaks of (u) symmetry in the XE spectra are slightly enhanced compared with spectra excited just above the onset of the ionization continuum. The results show that the third state has (u) symmetry for adsorption on both Cu and Ni. We conclude that this is a LUMO (e_{2u})-substrate hybrid.

The new occupied e_{2u} state appears differently in the spectra from benzene on Cu and Ni. In the case of adsorption on Ni (Fig. 5), the new π state is located 1.7 eV below the Fermi level and hence overlaps the Ni d band region. The fraction of adsorbate character of this state has to be of similar magnitude as that of the higher-binding-energy π orbitals since the observed emission intensity is of comparable strength. The origin of the e_{2u} state is easily understood in a simple frontier orbital picture. The interaction of the e_{2u} orbital with Ni d states results in an occupied bonding orbital observed in XE, and an empty antibonding orbital, the e_{2u}^* state observed in XA. The strong molecular character of the bonding e_{2u} state implies that the corresponding antibonding e_{2u}^* state has significant metal character. This is confirmed by the reduced intensity of the e_{2u}^* XA peak relative to the e_{2u} resonance in the gas-phase spectrum [30]. The formation of a single bonding state rather than a band suggests that the e_{2u} orbital interacts mainly with a narrow distribution of states, i.e. the Ni d band. For benzene adsorbed on Cu (Fig. 6), the new occupied e_{2u} orbital is located just below the Fermi level. There seems to be a cut-off at the Fermi level. The adsorbate character in this orbital is rather low. This is also reflected in the relatively strong peak from the antibonding orbital in the XA spectrum in Fig. 6. Our observations suggest that the unoccupied e_{2u}^* orbital interacts with a broad continuum of metal states and becomes broadened with a tail extending below the Fermi level. There is no distinct separation between the bonding and antibonding part.

The interaction between an electron level in the adsorbate and the band-like distribution of substrate levels has been separated into two extreme cases [31–33]. If the interatomic Coulomb interaction (the driving force for generating bonding and antibonding states) is smaller than the band width of the substrate states no well-separated bonding–antibonding states are formed; only a broadened adsorbate-induced resonance level is formed. If, on the other hand, the Coulomb interaction is larger than the band width, discrete bonding and antibonding states are obtained. The former situation represents a weak coupling case such as benzene on Cu whereas the latter corresponds to strong coupling as in benzene on Ni.

In the σ symmetry XE spectra in Figs. 5 and 6 (solid lines), we find, at binding energies larger than 5 eV, an orbital structure identical to the free molecule [14, 29]. In addition we find for benzene on Cu, Fig. 6, two new weak structures at binding energies below 5 eV. These structures appear at the same binding energies as the $1e_{1g}$ and e_{2u} orbitals seen in the π symmetry spectrum. We can anticipate some symmetry mixing due to rehybridization. For benzene adsorbed on Ni the σ symmetry spectrum is different. Here we find significant σ intensity all the way to the Fermi level, marked σ in Fig. 5. A simple admixture of σ and π states is not sufficient to explain the appearance of new σ states in the spectrum, since then we would expect a σ electron distribution which resembles the π states with a peak at 1.7 eV (the backbonding e_{2u} orbital). The 2p valence states parallel to the surface must therefore interact with the metal somewhat differently from the perpendicular 2p states. The band-like character of the σ states indicates a hybridization of benzene σ states with the broad Ni sp band in addition to the d band. Since the HOMO and LUMO σ orbitals involve C–H contributions we expect that the presence of these new states could affect the C–H bond. This might have direct implications for

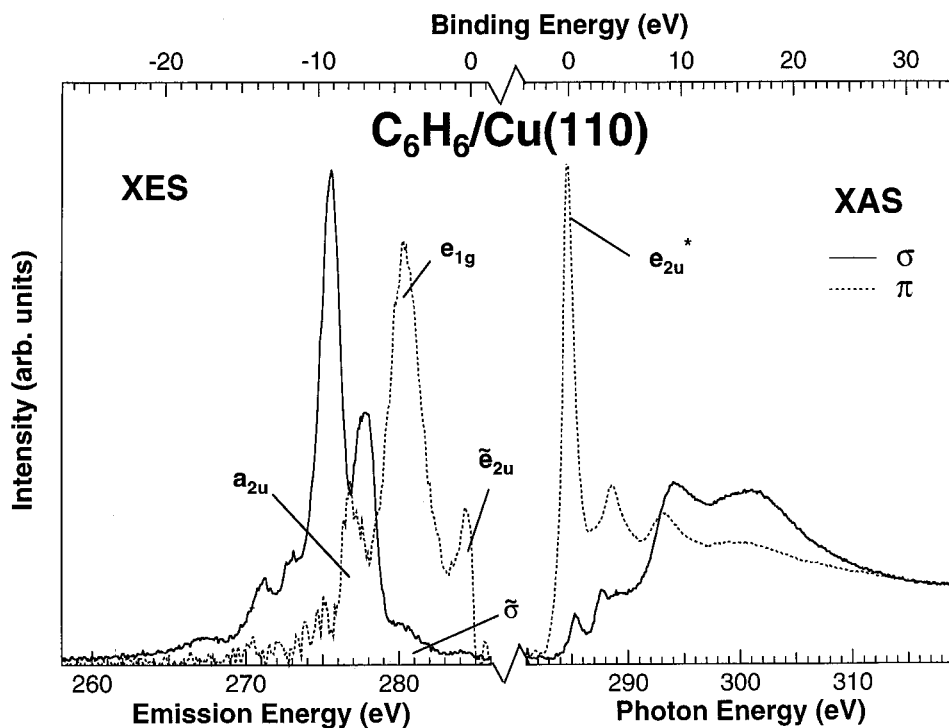


Fig. 6. Symmetry-resolved X-ray emission and X-ray absorption spectra for benzene on Cu(110). See Fig. 5

the important hydrogenation and dehydrogenation reactions of aromatic hydrocarbons on metal surfaces.

2.3 Glycine adsorbed on Cu(110)

The potential of XES applied to more complicated molecular adsorbates is well illustrated with glycine adsorbed on Cu(110). Glycine ($\text{HCOOCCH}_2\text{NH}_2$) is the simplest amino acid. Its properties are of biological interest. The molecule adsorbs with the molecular skeleton intact except for the removal of the acidic hydrogen. Figure 7 shows the orientation of the molecule on the Cu(110) surface [34]. The molecule is bonded to the surface through both the carboxylic group (COO) and the amino group (NH_2). The Cu(110) surface has a twofold symmetry, where the surface Cu atoms are oriented into rows in the [110] direction. The molecule adsorbs in an orientation perpendicular to these rows. From measurements of XE spectra in three directions (normal emission and grazing emission along the [110] and [100] directions), we can project the electronic structure on to the $2p_x$, $2p_y$, and $2p_z$ valence orbitals.

The two chemically different carbon atoms in the COO and CH_2 groups give rise to chemical shifted resonances in the X-ray absorption spectra. We may selectively excite each core level separately (similar to the N_2 on Ni case). Figure 7 shows XE spectra measured on four different atomic sites projected in three directions. The picture that emerges is an experimental version of the LCAO (linear combination of atomic orbitals) approach for molecular orbital theory. We can now study how molecular orbitals of a specific symmetry are distributed over different atomic sites in a complicated molecular complex. Combined with theoretical calculations, details of the chemical bond can be obtained from such studies.

3 Summary

The present paper demonstrates the application of the X-ray emission technique to the study of chemisorption systems. Such studies have become possible with the advent of high-brightness soft X-ray radiation from third-generation storage rings. It is clear from the examples presented that the technique provides a unique new insight into the nature of the surface chemical bond. The potential of the technique for the study of complex chemisorption systems involving molecules with different functional groups is also illustrated.

Acknowledgements. We thank the staff at the ALS for all their assistance. The support and valuable discussions with Nils Mårtensson, Joseph Nordgren, Lars Pettersson, and Hans Ågren are gratefully acknowledged. This research was sponsored by the Swedish Natural Science Research Council (NFR) and by the Göran Gustafssons Foundation for research in natural science and medicine.

References

1. N. Wassdahl, A. Nilsson, T. Wiell, H. Tillborg, L.C. Duda, J.H. Guo, N. Mårtensson, J. Nordgren, J.N. Andersen, R. Nyholm: *Phys. Rev. Lett.* **69**, 812 (1992)
2. H. Tillborg, A. Nilsson, T. Wiell, N. Wassdahl, N. Mårtensson, J. Nordgren: *Phys. Rev. B* **47**, 16464 (1993)
3. T. Wiell, H. Tillborg, A. Nilsson, N. Wassdahl, N. Mårtensson, J. Nordgren: *Surf. Sci.* **304**, L451 (1994)
4. A. Nilsson, P. Bennich, T. Wiell, N. Wassdahl, N. Mårtensson, J. Nordgren, O. Björneholm, J. Stöhr: *Phys. Rev. B* **51**, 10244 (1995)
5. A. Nilsson, M. Weinelt, T. Wiell, P. Bennich, O. Karis, N. Wassdahl, J. Stöhr, M.G. Samant, to be published
6. A.F. Starace: *Phys. Rev. B* **5**, 1773 (1972)
7. V.I. Grebennikov, Yu.A. Babanov, O.B. Sokolov: *Phys. Stat. Sol.* **79**, 423 (1977)
8. U. van Barth, G. Grossmann: *Phys. Rev. B* **25**, 5150 (1982)
9. A. Nilsson, N. Mårtensson: *Physica B* **208&209**, 19 (1995)

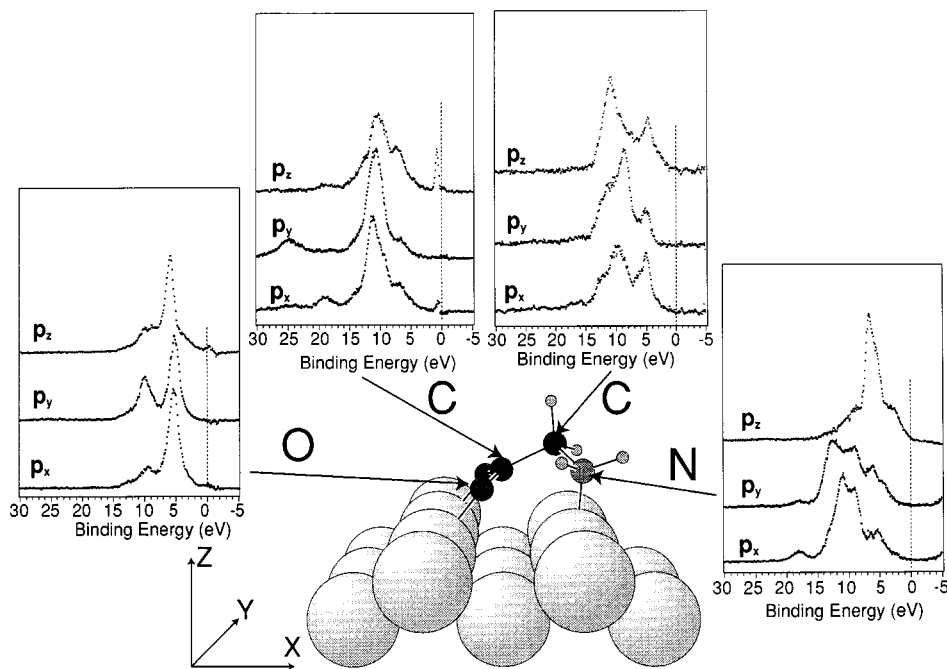


Fig. 7. $2p_x$, $2p_y$, and $2p_z$ symmetry-resolved X-ray emission spectra for glycine adsorbed on Cu(110). Inserted is a structural model of the adsorption complex [34]. The spectra are measured at the O atom, the C atom in the (COO) group, the C atom in the (CH₂) group, and at the N atom. The valence $2p_x$, $2p_y$, and $2p_z$ orbitals were obtained by a suitable linear combination of XE spectra measured in normal emission, grazing emission along the [110] direction, and grazing emission along the [100] direction

10. A. Nilsson, O. Björneholm, E.O.F. Zdansky, H. Tillborg, N. Mårtensson, J.N. Andersen, R. Nyholm: *Chem. Phys. Lett.* **197**, 12 (1992)
11. V. Caravatta, L.G.M. Pettersson, O. Vahtras, H. Ågren: *Surf. Sci.* in press
12. W. Wurth, C. Schneider, R. Treichler, E. Umbach, D. Menzel: *Phys. Rev. B* **35**, 7741 (1987)
13. A. Sandell, O. Björneholm, A. Nilsson, B. Hernnäs, J.N. Andersen, N. Mårtensson: *Phys. Rev. B* **49**, 10136 (1994)
14. P. Skytt, J. Guo, N. Wassdahl, J. Nordgren, Y. Luo, H. Ågren: *Phys. Rev. A* **52**, 3572 (1995)
15. P. Glans, K. Gunnelin, P. Skytt, J.H. Guo, N. Wassdahl, J. Nordgren, H. Ågren, F.Kh. Gel'mukhanov, T. Warwick, E. Rotenberg: *Phys. Rev. Lett.* **76**, 2448 (1996)
16. J. Nordgren, G. Bray, S. Cramm, R. Nyholm, J.E. Rubensson, N. Wassdahl: *Rev. Sci. Instrum.* **60**, 1690 (1989)
17. G. Blyholder: *J. Phys. Chem.* **68**, 2772 (1964)
18. A. Sandell, O. Björneholm, A. Nilsson, E. Zdansky, H. Tillborg, J. Andersen, N. Mårtensson: *Phys. Rev. Lett.* **70**, 2000 (1993)
19. A. Nilsson, H. Tillborg, N. Mårtensson: *Phys. Rev. Lett.* **67**, 1015 (1991)
20. C. Brundle, P. Bagus, D. Menzel, K. Hermann: *Phys. Rev. B* **24**, 7041 (1981)
21. K. Horn, J. Dinardo, W. Eberhardt, H.J. Freund, E.W. Plummer: *Surf. Sci.* **118**, 465 (1982)
22. O. Björneholm, A. Nilsson, E. Zdansky, A. Sandell, H. Tillborg, J.N. Andersen, N. Mårtensson: *Phys. Rev. B* **47**, 2308 (1993)
23. P.S. Bagus, G. Pacchioni: *Surf. Sci.* **278**, 427 (1992)
24. H. Antonsson, A. Nilsson, N. Mårtensson, I. Panas, P. Siegbahn: *J. Elec. Spectrosc. Relat. Phenom.* **54**, 601 (1990)
25. C.L. Allyn, T. Gustafsson, E.W. Plummer: *Solid State Commun.* **28**, 85 (1978)
26. R.J. Smith, J. Anderson, G.J. Lapeyre: *Phys. Rev. B* **22**, 632 (1980)
27. P. Skytt, P. Glans, K. Gunnelin, J. Guo, J. Nordgren, Y. Luo, H. Ågren, to be published
28. M. Weinelt, T. Wiell, J. Hasselström, O. Karis, N. Wassdahl, A. Nilsson, L.G.M. Pettersson, H. Ågren, J. Stöhr, M. Samant, to be published
29. W. Huber, H.P. Steinrück, T. Pache, D. Menzel: *Surf. Sci.* **217**, 103 (1989)
30. J. Stöhr: *NEXAFS Spectroscopy*, Vol.25 of Springer Series in Surface Science (Springer, Heidelberg 1992)
31. P.W. Anderson: *Phys. Rev.* **124**, 42 (1961)
32. D.M. News: *Phys. Rev.* **178**, 1123 (1969)
33. J.R. Schrieffer, D.C. Mattis: *Phys. Rev.* **140**, 1412 (1965)
34. J. Hasselström, O. Karis, M. Weinelt, N. Wassdahl, A. Nilsson, M. Nyberg, L.G.M. Pettersson, J. Stöhr, M. Samant, to be published